UCRL- 94624
PREPRINT

Measurements of Losses and Lasing Efficiency in GSGG:Cr,Nd and YAG:Nd Laser Rods

J. A. Caird
M. D. Shinn
T. A. Kirchoff
L. K. Smith
R. E. Wilder

This paper was prepared for submittal to
Applied Optics.

May 20, 1986

DISCLAIMER

MEASUREMENTS OF LOSSES AND LASING EFFICIENCY IN GSGG:Cr,Nd AND YAG:Nd LASER RODS*

J. A. Caird, M. D. Shinn, T. A. Kirchoff,
L. K. Smith and R. E. Wilder

Lawrence Livermore National Laboratory
P.O. Box 5508
Livermore, California 94550

ABSTRACT

Laser rods procured from four different vendors were examined in order to assess the state-of-the-art in GSGG:Cr,Nd crystal growth. Measurement techniques included spectrophotometry (for absorption loss), interferometry (for distortion), polarimetry (for birefringence), and laser resonator insertion. Free running laser efficiency measurements were also performed. The level of losses characteristic of currently available GSGG:Cr,Nd laser rods was generally found to be much higher than that of commercially grown YAG:Nd. The intrinsic lasing efficiency of the co-doped GSGG rods, however, was typically found to exceed that of the YAG:Nd rods by more than a factor of 2.

*Work performed by the Lawrence Livermore National Laboratory under the joint auspices of the U. S. Department of Energy under Contract No. W-7405-ENG-48 and the U. S. Department of Defense under Defense Advanced Research Projects Agency order #5358.

MEASUREMENTS OF LOSSES AND LASING EFFICIENCY IN GSGG:Cr,Nd AND YAG:Nd LASER RODS*

J. A. Caird, M. D. Shinn, T. A. Kirchoff,
L. K. Smith and R. E. Wilder

I. INTRODUCTION AND SUMMARY

In recent years there has been a strong increase in interest in new active crystalline laser materials. Much of this renewed interest is a result of the discovery of efficient sensitization of neodymium laser emission by codoping neodymium and chromium in various crystalline hosts.[1-10] A number of studies have indicated a factor of 2 improvement in lasing efficiency relative to YAG:Nd when flashlamp pumping is employed.[5-10] Furthermore, co-doped gadolinium scandium gallium garnet (GSGG:Cr,Nd) appears to have spectroscopic and thermo-mechanical properties which would make it an attractive alternative to YAG:Nd in many applications.[11]

It has also been recognized that some of these materials have the potential to be grown in large boules, without a strained central region, or core, by Czochralski pulling.[12] This possibility was strongly suggested by the industrial growth of core-free single crystals of GGG up to 11 cm in diameter.[13-15] A typical production GGG boule is shown in Fig. 1. Recent work performed under contract to LLNL has successfully demonstrated the growth of core-free boules of GSGG:Cr,Nd up to 2.5" diameter.[16] Core-free growth of laser crystals will permit the fabrication of laser devices with significantly larger clear apertures than is possible using crystals with core. It is evident, therefore, that GSGG:Cr,Nd has a significant additional advantage over YAG:Nd which has always been grown with core (to date).

Internal studies performed at LLNL have identified a number of applications which require efficient, high average power lasers at a wavelength near 1 μm. GSGG:Cr,Nd has been identified as the material

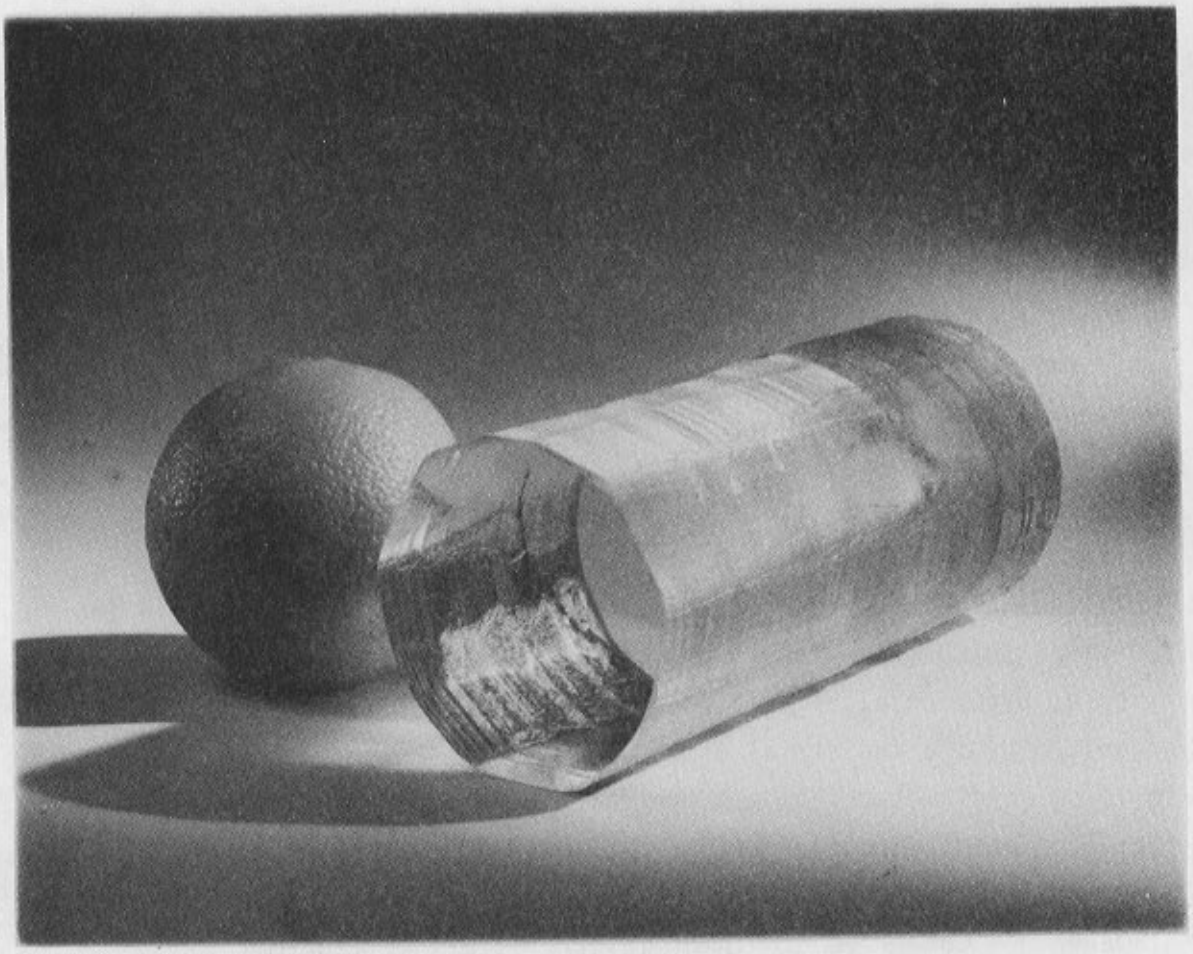

Fig. 1. Production boule of core-free GGG with 8-cm aperture and 25-cm length (Material Progress, Inc., Santa Rosa, Ca.).

which is most likely to meet these near term requirements if large crystals of adequate optical quality can be grown. Furthermore, this material can be used effectively to test the design principles and limitations of high average power slab lasers which are currently under study at this laboratory.

As a result of the above considerations an effort to advance the state-of-the-art in GSGG:Cr,Nd laser crystal growth was launched in 1984. In the first phase of this work we performed an evaluation of the status of the technology by procuring laser crystals from four commercial crystal growth companies. These were 1) Airtron, a Division of Litton Industries, Morris Plains, N.J., 2) Allied Technologies, Synthetic Crystal Products Division, Charlotte, N.C., 3) Material Progress, Inc., Santa Rosa, Ca., and 4) Union Carbide Crystal Products, Wasougal, Wa. Standard 0.25" diameter by 3" long GSGG:Cr,Nd laser rods were tested and compared with commercially available YAG:Nd rods as part of the evaluation process. The purpose of this document is to summarize the results obtained to date in the course of this testing program. The laser rods tested were procured under a number of different contracts and purchase orders with varying specifications, so that a direct comparison of each company's performance would not be meaningful. For this reason the vendor of each individual rod tested will not be identified in the summary of test results given in this report.

On the average it was found that losses in the GSGG:Cr,Nd rods exceeded those of YAG:Nd. This was not surprising, considering the number of years of experience that the laser industry has had with YAG crystal growth, and its relative inexperience with GSGG. Despite higher levels of loss it was found that the best GSGG:Cr,Nd rods yielded nearly twice the lasing efficiency of the best YAG:Nd rods when tested in a free running laser resonator, in agreement with earlier studies.[5-10]

On the basis of these results and on a favorable evaluation of the spectroscopic, optical, and thermo-mechanical properties of the material,[11] we have embarked on a new phase in its development. The emphasis of current efforts is on the reduction of losses to substantially lower levels and on scaling up the crystal growth process to a level consistent with application requirements.

II. CRYSTAL GROWTH

Most of the GSGG:Cr,Nd laser rods which were examined in the course of this work were fabricated from crystal boules which were grown under DOE or LLNL contracts. All crystals were grown by the Czochralski technique, but the growth conditions were somewhat varied, as were the stoichiometries of the melts. Some of the relevant crystal growth parameters are given in Table 1. The data in Table 1 were extracted from interim and final reports written under the aforementioned contracts.[16-20]

The laser rod dopant ion number densities reported in Table 1 were determined from the melt formulas using previously determined distribution coefficients of 1.00 ± 0.05 for chromium and 0.65 ± 0.05 for neodymium.[11] The quoted number densities refer to the top of the boule, or the first material to crystallize. The melt becomes enriched with neodymium as the crystal grows (due to the less than unity distribution coefficient), so the last material to crystallize has a slightly higher neodymium concentration. The ratio of the initial ion concentration in the crystal, C_i, to the final ion concentration, C_f, can be estimated from the relation[16]

$$\frac{C_i}{C_f} = (1-g)^{k-1} \qquad (1)$$

where k is the ion's distribution coefficient, and g is the fraction of the melt crystallized. Using this formula it is estimated that the increase in neodymium concentration was typically between 10% and 20% over the length of the crystals studied here.

III. SOURCES OF LOSS AND METHODS OF MEASUREMENT

While most GSGG:Cr,Nd rods tested during the course of these measurements exhibited significantly higher lasing efficiency than standard YAG:Nd rods, the results indicated a considerable variation in performance from rod to rod. These variations were larger than could be attributed to changes in doping concentrations. Not surprisingly, it was found that the major differences in laser performance were attributable to differences in crystal quality and the resultant variations in optical

Table 1. GSGG:Nd,Cr Melt Stoichiometries and Crystal Growth Conditions

Crystal #	Melt Composition[a] and resulting dopant densities[b] Gd	Nd [$10^{20}cm^{-3}$]	Sc	Cr [$10^{20}cm^{-3}$]	Ga	Boule Diameter (inches)	Pull Rate (mm/hr)	Rotation Rate (rpm)	Comments <111> growth axis and 2% O_2 in N_2 atmosphere unless otherwise indicated
1008	2.885	0.115 [3.0]	2.000	0.0072 [0.29]	2.993	1.2	1.0	2.5	<211> growth axis, deep interface
1035	2.917	0.083 [2.2]	1.950	0.050 [2.0]	3.000	1.8	1.0	2.5	<211> growth axis, deep interface
3002	2.9815	0.0505 [1.3]	2.0000	0.0225 [0.9]	2.9455	1.0	2.5	45	Spontaneously nucleated growth direction 15° off <100>, non-flat interface, CO_2/N_2 atmosphere
3003	2.9562	0.0758 [2.0]	2.0000	0.0225 [0.9]	2.9455	1.0	2.5	45	non-flat interface, CO_2/N_2 atmosphere
3004	2.9388	0.0762 [2.0]	1.9775	0.0225 [0.9]	2.9850	1.0	2.5	45	non-flat interface, CO_2/N_2 atmosphere
3006	2.9387	0.0933 [2.45]	2.0000	0.0225 [0.9]	2.9455	1.0	2.5	45	non-flat interface, heavy scatter, CO_2/N_2 atmosphere
3007	2.9562	0.0758 [2.0]	2.0000	0.0225 [0.9]	2.9455	1.0	5.0	48	non-flat interface, higher strain due to faster pull, CO_2/N_2 atmosphere
3008	2.9458	0.0692 [1.8]	1.8000	0.0495 [2.0]	3.1355	1.0	2.5	45	non-flat interface, composition adjusted toward assumed congruency, CO_2/N_2 atmosphere
3009	2.9558	0.0762 [2.0]	1.7200	0.0495 [2.0]	3.1985	1.0	2.5	45	non-flat interface, CO_2/N_2 atmosphere

Table 1. GSGG:Nd,Cr Melt Stoichiometries and Crystal Growth Conditions (Continued)

Crystal #	Melt Composition[a] and resulting dopant densities[b] Gd	Nd [$10^{20}cm^{-3}$]	Sc	Cr [$10^{20}cm^{-3}$]	Ga	Boule Diameter (inches)	Pull Rate (mm/hr)	Rotation Rate (rpm)	Comments <111> growth axis and 2% O_2 in N_2 atmosphere unless otherwise indicated
3010	2.9558	0.0762 [2.0]	1.8000	0.0495 [2.0]	3.1185	1.0	1.25	45	non-flat interface, CO_2/N_2 atmosphere
3011	2.9558	0.0762 [2.0]	1.8000	0.0495 [2.0]	3.1185	1.0	2.5	45	<110> axis, non-flat interface, heavy scatter where dendrites fell into melt, CO_2/N_2 atmosphere
3012	2.9558	0.0762 [2.0]	1.8000	0.0495 [2.0]	3.1185	1.0	2.5	45	<211> axis, non-flat interface, CO_2/N_2 atmosphere
4011	2.95	0.05 [1.3]	1.975[c]	.025 [1.0]	3.00	1	unk.	unk.	High strain due to fast pull (seed boule)
5001	3.03	0.084 [2.2]	1.87	0.05 [2.0]	3.00	1.0	1.5	up to 55	varied rotation rate to determine flat interface conditions (no rods fabricated
5002	3.03	0.084 [2.2]	1.87	0.05 [2.0]	3.00	1.0	variable	60	pull rate varied 3.0, 6.0 and 7.5 mm/hr, bubbles formed at 6.0 and 7.5 mm/hr (no rods fabricated)
5003	3.03	0.084 [2.2]	1.87	0.05 [2.0]	3.00	1.5	1.5	30	deep interface with core (no rods fabricated)
5004	3.03	0.084 [2.2]	1.87	0.05 [2.0]	3.00	1.5	1.5	43	flat interface

Table 1. GSGG:Nd,Cr Melt Stoichiometries and Crystal Growth Conditions (Continued)

Crystal #	Melt Composition[a] and resulting dopant densities[b] Gd	Nd [$10^{20}cm^{-3}$]	Sc	Cr [$10^{20}cm^{-3}$]	Ga	Boule Diameter (inches)	Pull Rate (mm/hr)	Rotation Rate (rpm)	Comments <111> growth axis and 2% O_2 in N_2 atmosphere unless otherwise indicated
5005	3.03	0.071 [1.85]	1.57	0.05 [2.0]	3.30	1.5	1.5	41	flat interface, dislocations composition adjusted toward assumed congruency
5006	2.95	0.071 [1.85]	1.95	0.05 [2.0]	3.00	1.4	1.5	47	flat interface, dislocations
5007	3.03	0.071 [1.85]	1.67	0.05 [2.0]	3.20	1.4	1.5	50	flat interface, no dislocations
5008	3.03	0.071 [1.85]	1.67	0.025 [1.0]	3.225	1.4	1.5	50	flat interface, no dislocations
5009	3.03	0.071 [1.85]	1.57	0.05 [2.0]	3.30	1.4	1.5	50	flat interface, CO_2/N_2 atmosphere, no dislocations
5010	3.03	0.071 [1.85]	1.57	0.05 [2.0]	3.30	1.4	1.5	53	reload, flat interface, CO_2/N_2 atmosphere, heavy dislocations
5014	3.03	0.074 [1.95]	-	0.0065 [1.0][d]	4.956	1.0	1.0	50	GGG, active Cr addition, heavy iridium inclusions, deep interface

[a] Based on 8 cations per crystal formula unit.
[b] Calculated assuming distribution coefficients of 1.0 for Cr and 0.65 for Nd.[11]
[c] We assume the crystal grower substituted Cr for Sc in this stoichiometric formula.
[d] Assumes Cr distribution coefficient is 3.5 in GGG.

loss. Therefore most of the testing program was designed to measure the effects of various types of loss in GSGG:Cr,Nd in comparison to YAG:Nd.

A number of different sources of loss were encountered during the testing program. The major sources were identified as:

1. Absorption by impurities and defects
2. Wavefront distortion due to refractive index inhomogeneity
3. Scattering from defects such as inclusions, voids, striations, etc.
4. Strain birefringence due to core, dislocations, striations, etc.
5. Intrinsic absorption from the lower laser level.

A number of different measurement techniques were used to characterize the laser rods under study. These included:

1. Twyman-Green interferometry at 1.06 μm
2. Circular polarimetry
3. Spectrophotometry
4. Diffraction limited transmission (or pinhole transmission) measurements
5. Laser resonator insertion (the Findlay-Clay technique).

The results of testing by the various techniques will be discussed in the following sections.

IV. TWYMAN-GREEN INTERFEROMETRY

The optical quality of the laser rods was tested using the Twyman-Green interferometer depicted in Fig. 2. All measurements were performed with cw YAG:Nd laser illumination since the GSGG:Cr,Nd laser rods do not transmit the red neon-helium laser wavelength. A lens was used to project the interference pattern onto the image plane of an infrared vidicon with appropriate magnification. The pattern was recorded by taking a polaroid photograph of the television monitor screen. A Zygo automatic pattern processor (ZAPP) was subsequently used to analyze the fringe patterns from the photographs.

The results of interferometry measurements on more than 20 laser rods are given in Table 2. Several GSGG rods showed high bulk distortion. These rods were almost all taken from 1 inch diameter boules which were grown with a non-flat melt/crystal interface and which therefore had a badly strained central core region. The bulk refractive index

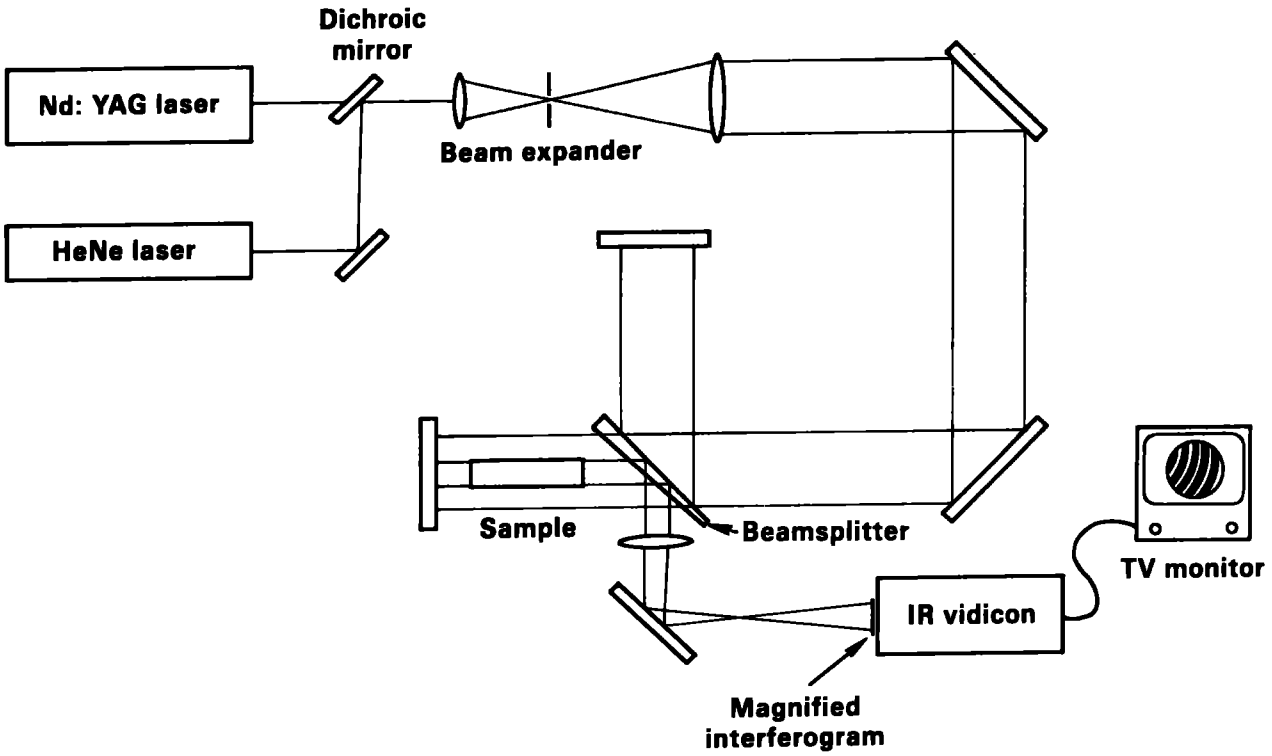

Fig. 2. 1 μm Twyman-Green interferometer with video display.

Table 2. Results of Interferometry and Birefringence Measurements

Crystal #	Wavefront Distortion Peak to Valley (waves)	Wavefront Distortion rms (waves)	Depolarization Loss (% cm^{-1}) Axial	Birefringence Δn_{rms} (nm/cm) Axial	Depolarization Loss (% cm^{-1}) Transverse	Birefringence Δn_{rms} (nm/cm) Transverse
1008	0.176	0.043	0.042	2.5	0.5 c	55 c
1035	0.163	0.027	0.016	1.5	0.2	33
3002	0.377	0.082	0.157	4.8	1.3	90
3003	0.677	0.170	0.182	5.2	5.9	172
3004	0.731	0.162	0.175	5.1	4.4	138
3006	0.360	0.047	0.046	2.6	11.1	245
3007	0.364	0.080	0.131	4.4	5.6	191
3008	0.655	0.144	0.563	9.2	1.2	87
3009	N/A[d]	N/A[d]	N/A[d]	N/A[d]	1.9	112
3010	0.429	0.099	0.048	2.7	0.4	44
3011	0.222	0.049	0.159	4.9	0.1	27
3012	0.271	0.066	0.200	5.5	0.5	49
4011	0.335	0.072	0.362	7.4	-	-
5001	-	-	-	-	3.7	169
5002	-	-	-	-	0.6	66
5003	-	-	-	-	1.0	77
5004-3	0.144	0.031	0.068	3.2	0.3	50
5004-4	0.092	0.019	0.015	1.5	0.3	50
5005	0.103	0.023	0.044	2.5	0.8 c	75 c
5007-2	0.200	0.041	0.014	1.4	0.2	35
5008	0.196	0.029	0.011	1.2	-	-
5009	0.178	0.037	0.002	0.5	1.0	86
5010	0.149	0.031	0.703	10.1	0.5 c	51 c
5014 b	0.805	0.150	1.53	14.5	-	-
0000 a	0.201	0.039	0.002	0.6	-	-
3013 a	0.132	0.029	0.012	1.3	-	-
4100 a	0.136	0.029	0.005	0.9	-	-

a = YAG:Nd Rods b = GGG:Nd,Cr Rod c = Average of 2 samples d = Intense absorption prevented measurement

inhomogeneity resulting from the strain in the crystal was responsible for the high distortion readings. Most of the rods showing low distortion came from 1.5 inch diameter boules which were grown with a flat melt/crystal interface and which were therefore core-free.

The results show that the optical quality of the GSGG:Cr,Nd laser rods tested was generally poorer than for high quality commercial YAG:Nd, but that with appropriate control of the crystal growth process it is possible to obtain co-doped GSGG with essentially equivalent optical quality. It is quite possible that GSGG:Cr,Nd can be more readily produced with optical quality higher than YAG:Nd because the former crystal can be grown with a flat melt/crystal interface while the latter cannot.

V. CIRCULAR POLARIMETRY

There are some instances where the state of polarization of a laser does not matter, but in many cases it is very important and depolarization must be treated like any other loss mechanism. It is important to avoid depolarization, for example, when polarizing optical elements are employed in a laser cavity or system. Furthermore, phase-matching in most nonlinear media can only be done with polarized beams, so that when harmonic generation is desired depolarization reduces the efficiency of frequency conversion.

Although the basic garnet crystal structure is cubic, with isotropic refractive index, imperfections in the structure often produce measureable levels of birefringence. The most common imperfections are inclusions (metallic and/or second phase), dislocations, striations, and facet strain. These imperfections create local stress, and optical anisotropy through the stress-optic effect. A measurement of birefringence, therefore, can be used as an indicator of the state of crystal perfection. It should be noted, however, that for certain types of imperfections the anisotropy generated has a special orientation relative to the direction of crystal growth. Therefore, the extent to which a beam will be depolarized on propagation through the material can depend strongly on the direction of propagation, and the polarization angle relative to the growth direction.

Inclusions are always accompanied by some degree of internal stress, which may be localized in the form of dislocation loops, or may take the form of extended dislocations which propagate through the crystal. In our experience, the inclusion density has to be very high before the birefringence they generate becomes excessive. The susceptibility of metallic inclusions to laser damage is probably a much more important concern than the birefringence they produce.

Dislocations can be generated at inclusions, or at any other point where a large amount of strain is present during the crystal growth process. When they form loops their effect is localized, and not as important as when they propagate through the crystal. Normally dislocations tend to propagate normal to the crystal/melt growth interface; hence their effects depend to some extent on the shape of that interface. If the growth interface is deep and (roughly) conical, as in YAG:Nd crystal growth, the dislocations will propagate out and terminate at the edge of the boule as the crystal grows. On the other hand, if the growth interface is flat (normal to the growth direction) the dislocations will propagate nearly parallel to the boule axis and their contribution to depolarization of light propagating in this direction is enhanced. A flat interface is desirable to produce "core-free" crystal growth (see below), but most Czochralski growth starts with a deep interface followed by a transition to flat interface growth. Under certain circumstances a large number of dislocations can be generated in the process of making the transition, so it becomes a particularly crucial step in the growth process.

Slight variations in the composition of the growing crystal are caused by more or less random fluctuations in the growth rate combined with gradients in composition of the melt near the interface (due to non-unity distribution coefficients of the melt's constituents).[21] The changes in composition produce slight changes in the lattice parameter of the crystal, which creates strain between adjacent regions that grew at different rates.[22] The changes occur in layers which replicate the shape of the crystal/melt growth interface, and which are commonly known as striations. On a microscopic scale the striations appear locally planar, with properties which are rotationally invariant with respect to the normal to these planes. Thus the material becomes locally uniaxial,

with the local optic axis perpendicular to the planes of striation. Depolarization due to striations is minimized, therefore by propagation normal to them, or by choosing a polarization which is either parallel or perpendicular to the plane of incidence on them. For boules grown with a flat interface depolarization due to striations is minimized by propagation parallel to the boule axis (perpendicular to the growth interface).

It has been shown that striations can be minimized through the use of a congruently melting crystal stoichiometry.[23] A number of different stroichiometries were tried in the course of this work as was discussed in Section II. At this time, it is not known how close any of these formulas came to the congruently melting GSGG composition.

Strain is also created at the junction between crystal facets which tend to grow at different rates, and with slightly different compositions.[24,25] This effect is most readily seen in the center of a Czochralski grown boule where a number of facets come together to form a highly strained "core". Core-free crystals can be obtained by maintaining a flat interface between the growing crystal and the melt. The flat interface can be in the direction of a single natural facet of the crystal, or in a direction where no natural facet forms. Core-free growth increases the yield of laser rods which can be cut from a crystal boule, and is essential to the production of high optical quality slab laser plates with maximum ratio of plate to boule dimensions.

Depolarization losses and r.m.s. birefringence ($\Delta n_{r.m.s.}$) values were measured with the polarimeter shown schematically in Fig. 3. Circularly polarized light was used to minimize any effects due to sample orientation. The fraction of beam energy converted from one state of polarization to the other is equal to $\sin^2(\phi/2)$ where ϕ is the phase angle of retardation. For small ϕ, the loss fraction is equal to $\phi^2/4$. In a nominally isotropic material, it is supposed that the retardation will vary randomly, with a spatially averaged value of zero. The spatially averaged r.m.s. retardation will scale with the square root of the propagation distance (resulting from the random walk process). The net loss due to depolarization should therefore scale linearly with propagation distance. The measurements described in this report are therefore given in terms of depolarization loss per unit length.

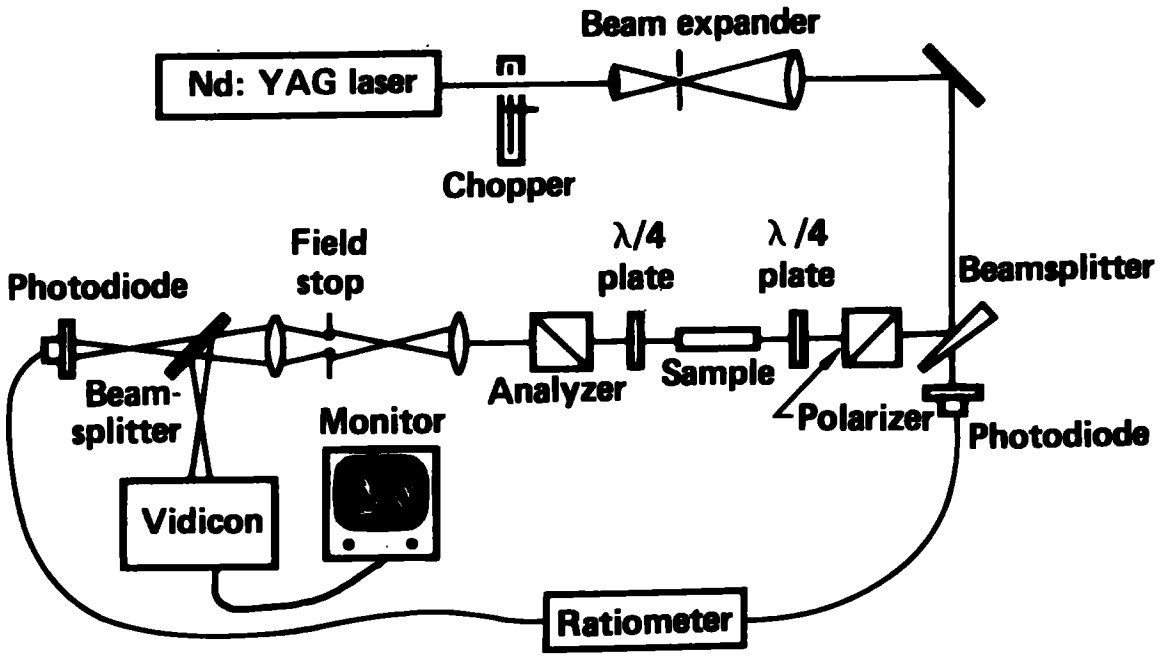

Fig. 3. Circular polarimeter for birefringence measurements.

A commonly quoted parameter for materials with constant retardation per unit length, is the index difference, Δn, which is related to the retardation phase angle by

$$\Delta n = \frac{\phi}{2\pi} \frac{\lambda}{\ell} \tag{2}$$

where ℓ is the propagation distance. If ϕ is spatially nonuniform, the intensity in the polarization orthogonal to the input polarization is proportional to the spatially averaged mean value of ϕ^2 (for small values of ϕ). In such cases it makes sense to define an r.m.s. value of Δn,

$$\Delta n_{r.m.s.} = \frac{\lambda}{2\pi\ell} \phi^2_{mean} \quad . \tag{3}$$

This value will be quoted along with the measured values of depolarization loss per unit length. However, considering the arguments presented in the preceding paragraph it would be inappropriate to use $\Delta n_{r.m.s.}$ as if it were a constant in loss calculations.

A reference signal was generated by placing a linear polarizer in the position of the sample. Let ϕ be the phase angle of retardation induced by a sample of spatially uniform birefringence. It can be shown that the ratio of the signal generated by such a sample to that obtained using the linear polarizer is equal to ϕ^2 (for $\phi<\pi/4$). For samples with non-uniform birefringence, the sample to reference signal ratio is equal to the spatially averaged or mean value of ϕ^2. The experimentally determined depolarization loss coefficient is given by

$$\alpha_{dp} = \frac{\phi^2_{mean}}{4\ell} \tag{4}$$

where ℓ is the length of the sample. The value of r.m.s. birefringence was then obtained by using Eq. 3. Results for axial propagation through each laser rod tested are presented in Table 2.

A reasonable tolerance for birefringence loss is on the order of 1×10^{-3} cm^{-1}, depending on the application and specific laser system design. The measurements described here indicate that about half of the GSGG rods tested would meet the stated tolerance. All of the YAG:Nd rods measured were found to be an order of magnitude better than this. For GSGG, the most consistently good results were obtained for rods cut from flat interface boules. One of the GSGG rods showed a depolarization loss coefficient lower than any of the YAG rods tested. Crystal #5010 was a flat interface boule, but the rod had a high level of birefringence due to a high density of dislocations.

The rods cut from non-flat interface boules showed much higher levels of birefringence in addition to the higher levels of bulk distortion discussed in Section IV. These boules exhibited a strained core and striations which were not generally normal to the direction of propagation. An additional factor which may have contributed to the high levels of strain in these crystals was a higher growth rate (typically 2.5 mm/hr.). The crystals exhibiting low levels of birefringence were typically pulled at 1.5 mm per hour or slower.

Whenever possible a window sample was cut out of each boule from which a laser rod had been fabricated. The windows were oriented with surfaces parallel to the boule growth axis. These samples were used to measure the r.m.s. birefringence for propagation normal to the boule axis, and roughly parallel to the growth striations. The results are also reported in Table 2 for comparison. The losses which will be experienced in a properly engineered laser system (polarization parallel or perpendicular to the plane of incidence on the striations) should be similar to our axial propagation measurements described in the preceding paragraphs, and not to the measurements for propagation normal to the boule axis.

The measurements of depolarization for transverse propagation are qualitative in nature due to moderate fluctuations in their intensity from point to point in the samples. However, some general conclusions can still be drawn from the results. The series of crystals 3002 to 3012 shows the dramatic effect of melt composition on birefringence due to striations. These samples are shown as viewed simultaneously between crossed polarizers in Fig. 4. Crystals 3002 to 3007 were grown from

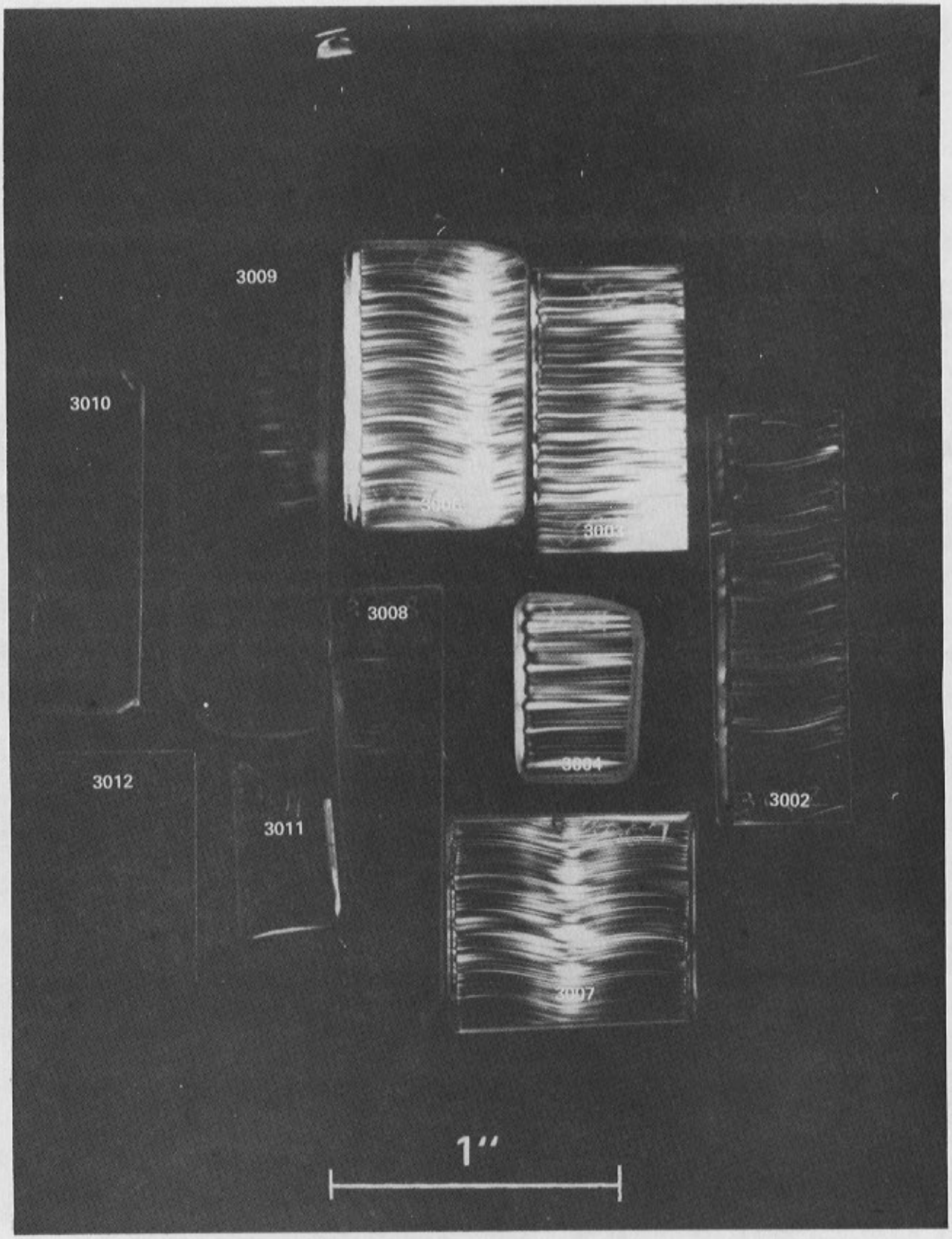

Fig. 4. Windows cut parallel to the boule growth axis for crystals 3002 to 3012, as viewed simultaneously between crossed polarizers.

melts of very similar stoichiometry, and all show relatively high birefringence due to striations. The melts for crystals 3008 to 3012 used about 10% less scandium, and were thought to be more nearly congruently melting. The depolarization loss for transverse propagation is seen to be about an order of magnitude less for the latter series of crystals.

Another interesting effect is seen by comparison of the results for crystal 3002 with those for crystals 3003 to 3007. Here, the melt stoiciometries are nearly the same, as are most of the other growth parameters, except for crystallographic orientation. Crystals 3003 to 3007 were grown along a <111> crystallographic axis, while crystal 3002 accidentally nucleated in a direction about 15 degrees off a <100> axis.[19] Crystal 3002 shows significantly less transverse birefringence than the others in the series. This may indicate that the direction of crystal growth can also have a strong effect on the level of strain and depolarization loss which is produced in the crystal. A similar effect could explain the substantially lower striation birefringence in crystal #3011, grown along <110>, compared to other crystals in the 3008 to 3012 group which were grown along the <111> or <211> axes.

VI. SPECTROPHOTOMETRY

A number of the GSGG:Cr,Nd crystals grown as part of this project were found to exhibit an absorption band in the near infra-red stretching from about 850 to 1200 nm (centered near the desired 1 μm laser wavelength). The strength of the absorption varied significantly from sample to sample, and was often strong enough to affect lasing efficiency, or to prevent laser action at 1061 nm altogether. The absorption spectrum of a crystal exhibiting this effect is shown in Fig. 5. After a long series of analytical chemistry studies we were able to establish a correlation between the strength of this absorption and the level of calcium impurity in the crystal,[26] as shown in Fig. 6. Our current hypothesis is that the divalent calcium causes chromium to switch from the +3 to +4 valence state if it is not otherwise compensated by +4 impurities.[27] Cr^{4+} on a tetrahedral site in the crystal is thought to produce the near infra-red absorption band.

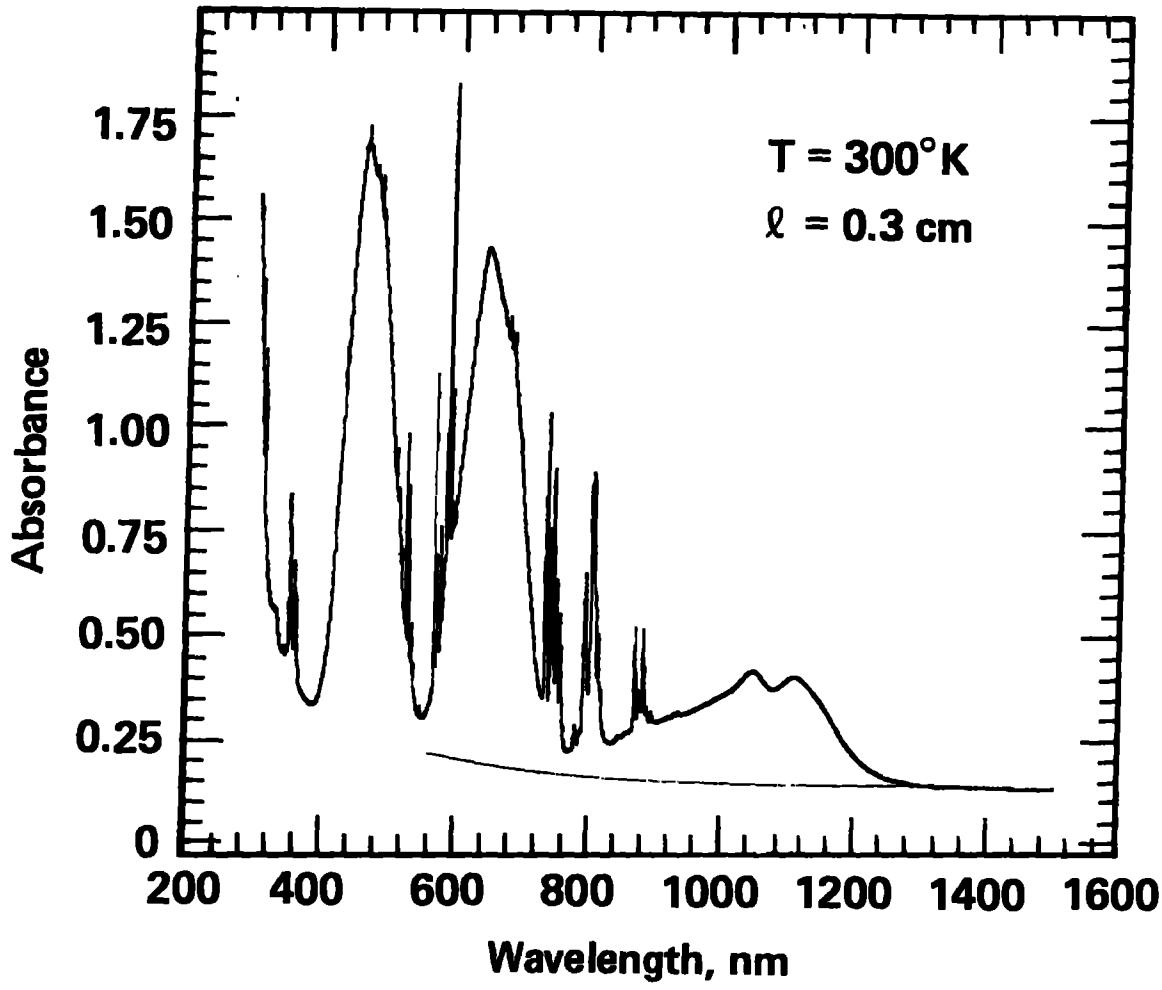

Fig. 5. Absorption spectrum of a GSGG:Cr,Nd crystal grown after about 100 wt. ppm of calcium oxide was added to the melt.

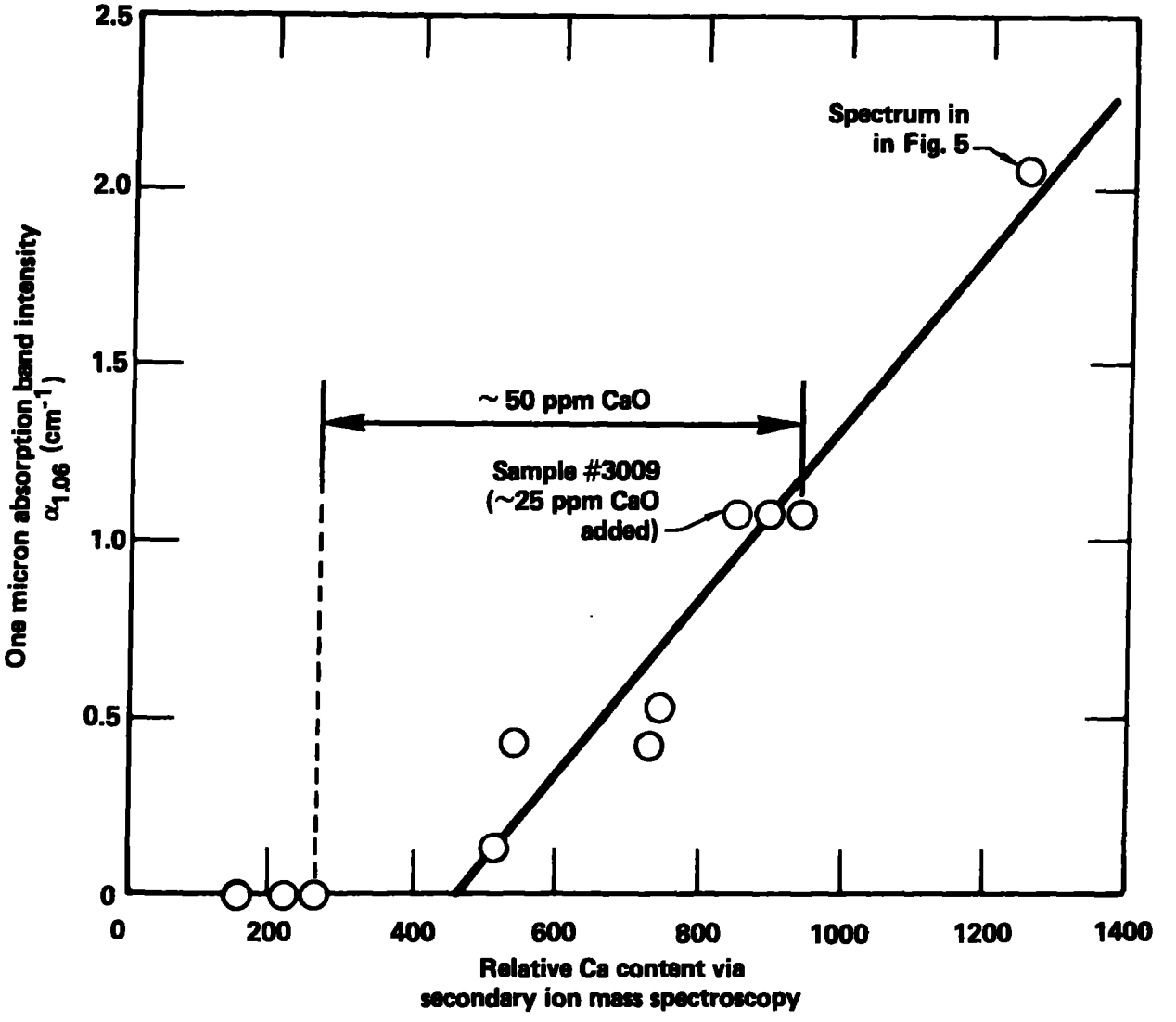

Fig. 6. Absorption coefficient at 1120 nm vs. calcium content of GSGG:Cr,Nd crystals as determined by secondary ion mass spectroscopy. Two of the crystals (indicated) were grown from the same melt, one before and one after the addition of 50 wt. ppm of CaO to the melt.[16]

Fortunately, most of the crystals we have received had acceptably low absorption coefficients at the 1061 nm laser wavelength, indicating that an appropriate impurity charge balance can be readily achieved. However, crystal growers will occasionally add on the order of 50 wt. ppm of calcium oxide to the melt to "promote the growth" of gallium garnet crystals (although it is not understood why this is necessary). Two of the data points shown in Fig. 6 were obtained from crystals grown from the same melt before and after 50 wt. ppm of calcium oxide was added. It was reported that 25 wt. ppm of calcium oxide was added to the melt for crystal #3009[19], also shown in Fig. 6. Chemical analysis of the starting materials used in the production of GSGG revealed the presence of calcium as a major impurity in most batches of scandium oxide tested (>100 ppm, typically). The other starting materials had very little calcium by comparison. We have made arrangements with Ames National Laboratory (Ames, Iowa) to refine future batches of Sc_2O_3 to roughly 10 ppm of Ca impurity.

In order to better determine the sources of loss at the lasing wavelength, the transmission spectrum of all laser rods was measured using a Perkin-Elmer Lambda 9 double beam spectrophotometer with a LLNL-built fixture, which held the laser rod parallel to the propagation axis of the sample beam. This insured that a high degree of measurement repeatability was maintained. The transmission measurements at 1064.5nm, using this arrangement, agreed to within ± 1% of the values obtained by insertion of the rods in the beam of a cw YAG:Nd laser. Thus, the measurements are believed accurate to about ± 0.15%cm^{-1}.

The total attenuation, measured at 1064.5nm, is given in the third column of Table 3. In most of the rods studied there was no Cr^{4+} absorption detectable above the baseline of the spectrophotometer trace. For those cases where Cr^{4+} absorption was detectable, an attempt was made to separate the contribution of the Cr^{4+} absorption from the baseline. This was achieved by comparing the spectrum of the rod with Cr^{4+} absorption to the baseline exhibited by a rod without the Cr^{4+} absorption. The values obtained from this method are given in columns one and two of Table 3. The error in the calculation is approximately ± 0.1%cm^{-1}. Baseline shifts due to imperfect A/R coatings are estimated to amount to less than 0.1%cm^{-1} for all rods measured.

Table 3. Results of Transmission Loss Measurements
(Spectrophotometric and Pinhole Transmission)

Crystal #	Spectrophotometer Measurements			250μrad Pinhole
	Baseline shift (%cm^{-1})	1μm Band (%cm^{-1})	Total (%cm^{-1})	Transmission Loss (%cm^{-1})
1008	0.5	0	0.5	1.8
1035	0.5	3.8	4.3	3.7
3002	0.8	0	0.8	3.1
3003	0.8	0	0.8	4.5
3004	0.8	0	0.8	8.5
3006	0.4	0	0.4	0.9
3007	0.45	0.45	0.9	3.6
3008	0.5	0	0.5	3.9
3009	N/A[c]	110	110	N/A[c]
3010	0.5	0	0.5	2.4
3011	0.8	0	0.8	1.5
3012	0.5	0	0.5	5.1
4011	0.7	0.2	0.9	4.3
5004-3	0.15	0.65	0.8	1.0
5004-4	0.4	0.8	1.2	0.9
5005	0.4	0	0.4	0.2
5007-2	0.4	0.6	1.0	1.3
5008	0.4	0	0.4	0.3
5009	0.5	0	0.5	0.5
5010	0.2	0	0.2	0.5
5014[b]	1.1	1.0	2.1	11.6
0000[a]	-	-	-	0.5
3013[a]	0.3	0	0.3	1.1

[a] YAG:Nd rods, [b] GGG:Cr,Nd rod
[c] Intense absorption prevented measurement.

The major sources of the baseline changes seen with different samples are thought to be due to a) absorption due to trace impurities, and b) large angle scattering (or absorption) by inclusions, voids or other defects in the crystal. The latter effect was clearly seen in crystal 5014, which contained a large number of iridium inclusions (see Table 3). Due to the large acceptance angle of the spectrophotometer detection system the losses due to small angle scattering cannot be determined on the basis of this data.

Thus, while the spectrophotometric technique provides useful data on the wavelength dependence of losses, it is not sensitive to all types of scattering mechanisms which can produce losses in a laser medium. Consequently, low loss values obtained using a spectrophotometer should be considered necessary, but not sufficient to insure that high efficiency will be achieved in a laser system.

VII. DIFFRACTION LIMITED TRANSMISSION MEASUREMENTS

Losses due to small angle scattering can be important whenever it is desired to produce a diffraction limited laser beam. When harmonic generation is required small angle scattering can also significantly affect the overall system efficiency because the harmonic conversion efficiency often depends strongly on the angle of incidence on the nonlinear material. Normal transmission measurements are inadequate to measure these losses because of the large acceptance angle of the detection system. For this reason, we designed and built the diffraction limited transmission measurement system depicted in Fig. 7. It should be noted that this apparatus measures the net loss due to absorption, scattering, and distortion at the diffraction limit of the chosen circular aperture size.

A cw YAG:Nd laser was chopped to allow synchronous detection. The beam was then expanded by a recollimating telescope in order to uniformly illuminate the sample with a plane wave. After passage through the sample the beam was made to diffract from a circular aperture. The beam was then reflected back through the sample a second time to increase the sensitivity of the measurement.

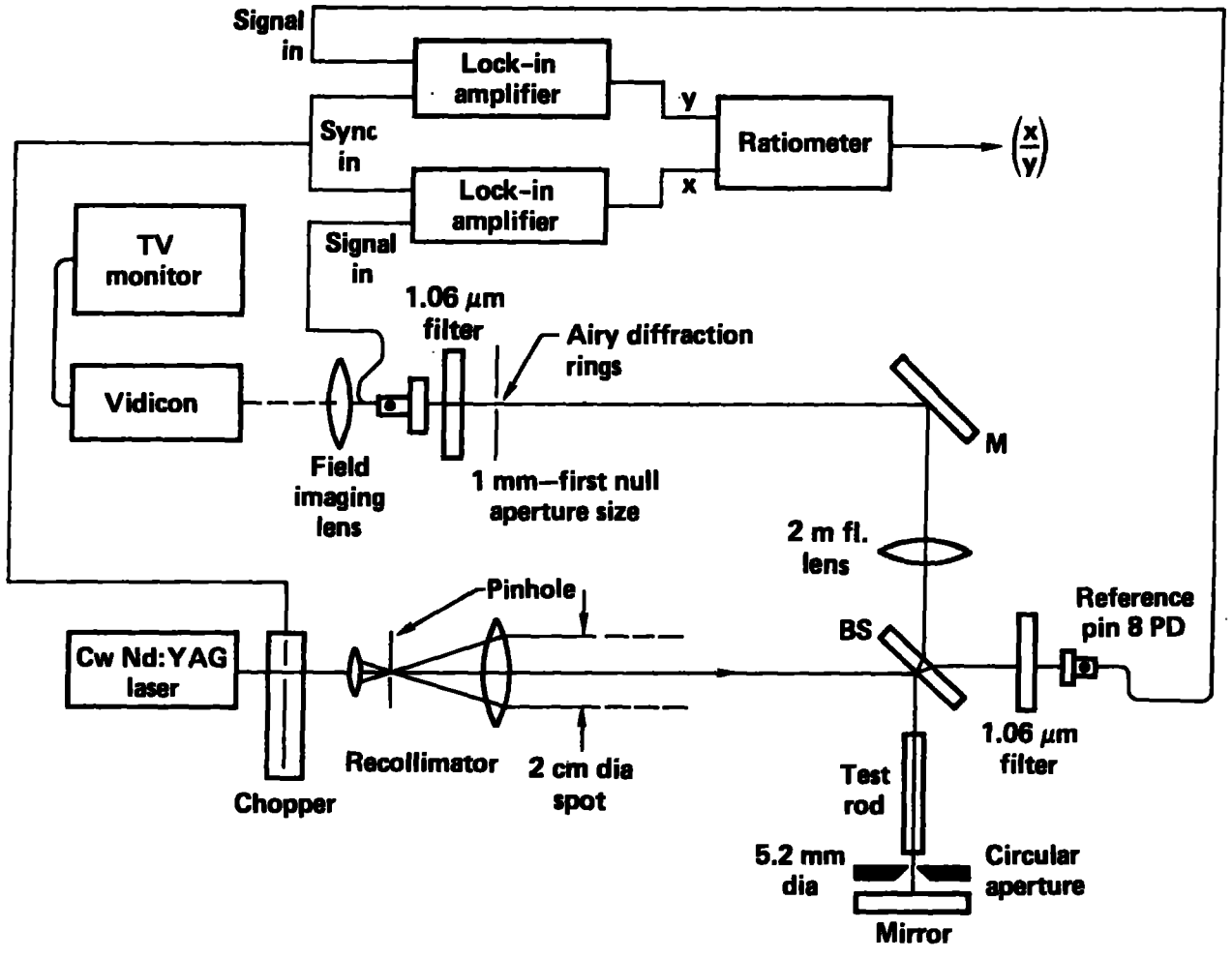

Fig. 7. System for measurement of diffraction limited transmission of test samples.

The circular aperture size must be somewhat smaller than the sample size, but large enough to produce the desired diffraction limited spot size. For the 0.25 inch diameter laser rods studied here, a 5.2 mm diameter aperture was used. In the far field this produced an Airy diffraction pattern with its first null at an angle of 250 μrad off axis. A 2 m focal length lens was used to generate the far field pattern, and a 1 mm diameter field stop (pinhole) was used to allow only the central spot intensity to be detected. The inside edge of the field stop was chosen to be at a null in the diffraction pattern in order to reduce the sensitivity of the measurement to angular misalignment. When aligning the system, the detector is removed, and a television monitor was used to view the far field pattern.

A reference measurement was made first, with no sample in the beam, and the amplifier gains were adjusted to give a reading of 1.000 on the ratiometer. The sample was then inserted, the system was realigned to eliminate the effect of any sample wedge, and a new reading was taken. If the far field pattern was badly distorted by the sample the alignment of the system was adjusted to give the maximum possible transmitted signal. The loss coefficient was obtained by taking the negative of the natural logarithm of the second reading and dividing by twice the length of the sample. All samples were antireflection coated so that no correction for the Fresnel reflectivity of the surfaces was necessary.

The results of our measurements on over 20 laser rods are given in Table 3. Several GSGG:Cr,Nd rods showed very high loss coefficients due to bulk distortion when tested in this manner (note the strong correlation between the pinhole loss coefficient and the levels of distortion determined interferometrically). These rods were almost all taken from 1 inch diameter boules which were grown with a non-flat melt/crystal interface and which therefore had a badly strained central core region. The bulk refractive index inhomogeneity and strain in the crystal were responsible for the high loss readings by this method of measurement. The rods giving low loss readings almost all came from 1.5 inch diameter boules which were grown with a flat melt/crystal interface and which were therefore core-free. These were also characterized by low refractive index inhomogeneity and beam distortion.

In the absence of distortion, it should be possible to equate the difference between the pinhole transmission measurements and the spectrophotometer transmission measurements (section VI) to small angle scattering. Unfortunately, distortion effects were quite large in a majority of the rods examined. However, in rods where distortion effects were small, the two types of transmission measurements usually gave comparable results (most often equal, to within the experimental error). On the basis of these experiments, therefore, we conclude that the effects of small angle scattering (>250 μrad) are on the order of, or less than the uncertainty in our measurements (~±0.2% cm^{-1}).

VIII. LASER RESONATOR INSERTION LOSS (FINDLAY-CLAY) MEASUREMENTS

The measurement methods described in Sections IV through VII are useful for providing a general characterization of the laser materials being tested. They may also be useful in estimating the performance of the material in certian specific applications. However, when a laser rod is used as the active element in an optical resonator, or oscillator, the round trip resonator losses are a complex function of the contributions of all of the loss mechanisms, and the optical design of the resonator. Furthermore, it is precisely these resonator losses which affect the operating efficiency of such a laser. When comparing lasing efficiency for different rods in the same laser resonator it is possible to measure and account for the net resonator losses in order to estimate the ultimate efficiency which could be obtained if the losses were eliminated. A comparison of the intrinsic efficiency potential of different laser rods is then obtained independent of the optical quality of the material.

A useful method for measuring laser resonator losses was first suggested by Findlay and Clay.[28] In their method, the threshold for laser oscillation in a particular laser resonator is measured as a function of the reflectivity of the output coupler, which is varied by changing mirrors. In a free running laser resonator, the threshold condition for laser oscillation can be expressed as

$$R_{out} \exp [2(\sigma N_{th} - \delta)\ell] = 1 \qquad (5)$$

where R_{out} is the reflectivity of the output coupler, N_{th} is the population density in the excited state at threshold, δ is the loss per unit length, and ℓ is the length of the laser rod. Taking the natural log of this equation yields

$$2\sigma N_{th}\ell - 2\delta\ell = -\ell n\, R_{out} \qquad (6)$$

Thus, a plot of N_{th} versus $\ell n\, R_{out}$ yields a straight line for which the round trip resonator loss, $2\delta\ell$, equals the extrapolated value of $\ell n\, R_{out}$ at $N_{th} = 0$.

Fortunately, in the Findlay-Clay analysis, it is not necessary to know the inversion density in absolute terms. Any signal or quantity that is proportional to the N_{th} can be measured and used. Findlay and Clay proposed the use of the pre-shot energy in the capacitor bank of the flashlamp pulse forming network (PFN) as a quantity that should be proportional to the inversion density. This method was attempted at Livermore, but systematic errors were encountered, especially at low input energy where the data are most important. Major discrepancies appear to arise when a reasonable fraction of the stored electrical energy is consumed in the lamp-ignition process. Errors can also arise because the pump pulse width is not a constant, independent of pulse energy.

In order to avoid these systematic errors the 1.3 μm fluorescence from the laser rod was used to produce a signal proportional to the excited-state density. The experimental arrangement[29] is shown in Fig. 8. The pump cavity was a close coupled, monolithic KSF-5 samarium glass structure, with diffusely reflecting walls (Kigre model #FC-25). The flashlamps had cerium-doped quartz envelopes. M_1 is the output coupler with reflectivity R_{out}, which is varied by changing out this mirror. M_2 is the rear resonator mirror, with ~100% reflectivity at 1.06 μm, but very high transmission (T>90%) at 1.3 μm. The fluorescence was imaged through a field stop onto an InAs detector cooled to liquid-nitrogen temperature. A narrow-band filter was also used to filter out 1.06 μm signals and to reduce any effect of scattered flashlamp light. A small correction factor was used to account for

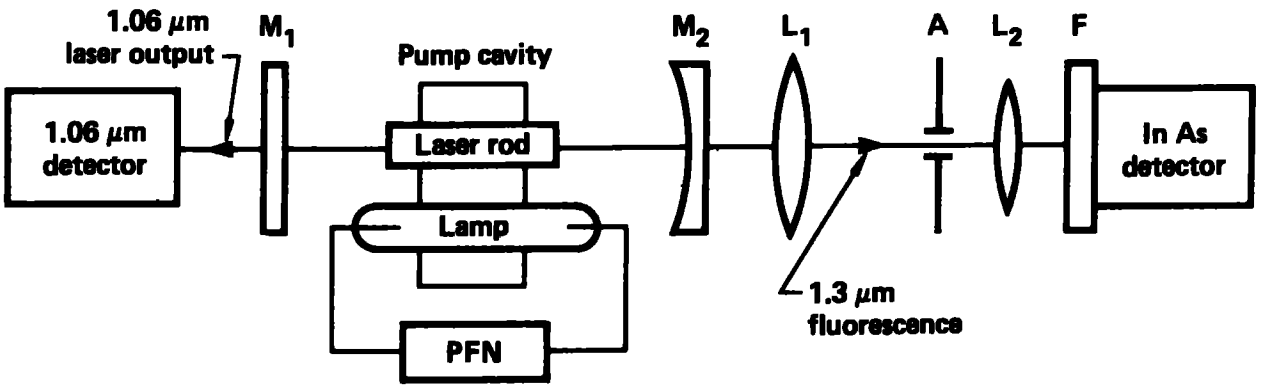

Fig. 8. Laser resonator for insertion loss (Findlay-Clay) and free running laser efficiency measurements.[29] M_1 is the output coupling mirror with reflectivity R_{out} at 1.06 μm; M_2 is a 1 m radius mirror with high reflectivity at 1.06 μm, and high transmission (> 90%) at 1.3 μm; L_1 is a 25 cm focal length lens; A is an aperture-field-stop at the laser rod image plane; L_2 is a 7.5 cm focal length lens; and F is a 1.3 μm narrow-band-pass filter.

signal variations caused by changes in the 1.3 μm reflectivity of the output coupler M_1.

The results of the Findlay-Clay loss measurements on four 0.25" diameter by 3" long GSGG:Cr,Nd laser rods obtained from the four different vendors, and one YAG:Nd laser rod of the same size are shown in Fig. 9. As indicated above, the resonator's round trip loss factor, $L = 2\delta\ell$, is equal to the value of the horizontal axis intercept for the straight lines drawn through the data. The losses measured for these and a number of other rods are given in Table 4. The lowest loss was obtained for a YAG:Nd rod, with a round-trip loss of 5%, or 0.3% cm^{-1}. The best GSGG:Cr,Nd rod measured to date yielded a round trip loss of 11%, or 0.7% cm^{-1}.

IX. FREE RUNNING LASER EFFICIENCY MEASUREMENTS

The laser resonator depicted in Fig. 8 was also used as a free running oscillator to measure the lasing efficiency for each laser rod. The input/output energy curves for one of the best performing GSGG:Cr,Nd rods and a high grade commercial YAG:Nd rod tested in the same resonator are shown in Fig. 10. The best results were usually obtained with an output coupler reflectivity of about 40%, and are given in Table 4 for all rods tested.

It can be shown within a reasonable approximation that the measured slope efficiency, η_s, is related to the resonator insertion loss parameter, $L = 2\delta\ell$, and the output coupler reflectivity, R_{out} by the expression[30]

$$\eta_s = \eta_o \ell n R_{out} / (\ell n R_{out} - L) \qquad (7)$$

where η_o is the intrinsic slope efficiency which could be obtained from each rod if all sources of loss were eliminated. Thus, the intrinsic slope efficiency for the laser material in each rod (as used in this laser resonator) can be determined using the measured slope efficiencies reported here and the Findlay-Clay resonator insertion loss parameters presented above, independent of the rod's optical quality. The calculated intrinsic slope efficiencies are given in Table 4.

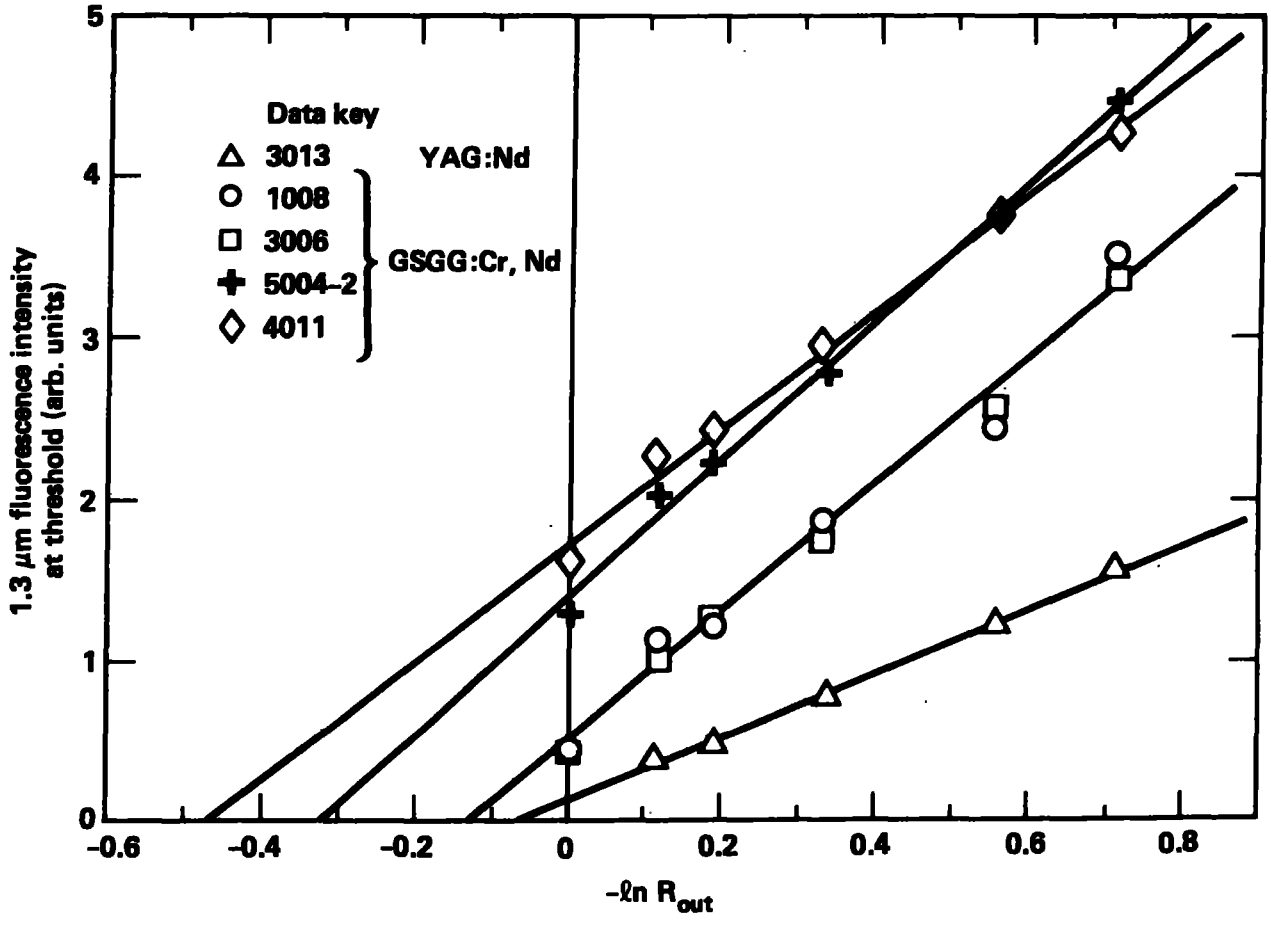

Fig. 9. Findlay-Clay insertion loss plots for four GSGG:Cr,Nd laser rods, and one YAG:Nd laser rod.[29]

Table 4. Laser Resonator Insertion Loss (Findlay-Clay), and Free Running Laser Efficiency Measurements. Estimates of Intrinsic Slope Efficiency Were Calculated Using Eq. 7.

Crystal #	Resonator Insertion Loss, L = 2ℓ	Loss Per Unit Length $\delta(cm^{-1})$	Efficiency Measurements (Rout = 40.8%) Absolute (%)	Slope (%)	Intrinsic (%)
1008	0.13	0.9	3.8	5.5	6.3
1035	0.81	5.3	2.8	4.2	8.0
3002	0.14	0.9	3.8	5.3	6.1
3003	0.20	1.3	4.6	6.6	8.1
3004	0.21	1.4	4.4	6.2	7.6
3006	0.12	0.8	4.6	6.5	7.4
3007	0.51	3.3	3.1	4.8	7.5
3008	0.12	0.8	4.9	7.0	7.9
3009	N/A[c]	110. [c]	N/A[c]	N/A[c]	N/A[c]
3010	0.18	1.2	4.7	6.7	8.0
3011	0.19	1.3	4.6	6.5	7.9
3012	0.14	0.9	4.8	7.1	8.2
4011	0.47	3.1	3.3	5.0	7.7
5004-3	0.36	2.3	4.4	6.2	8.7
5004-4	0.33	2.0	4.2	6.0	8.2
5005	0.13	0.8	4.8	6.8	7.7
5007-2	0.23	1.4	3.7	5.4	6.7
5008	0.11	0.7	4.6	6.6	7.4
5009	0.16	1.0	4.2	6.1	7.2
5010	0.12	0.8	5.0	7.0	7.9
5014 b	0.64	4.0	2.7	4.3	7.3
0000 a	0.08	0.6	2.2	3.1	3.4
3013 a	0.05	0.3	2.8	3.6	3.8
4100 a	0.08	0.5	2.2	3.0	3.2

a = YAG:Nd rods
b = GGG:Cr,Nd rod
c = rod did not lase due to strong 1μm absorption band.

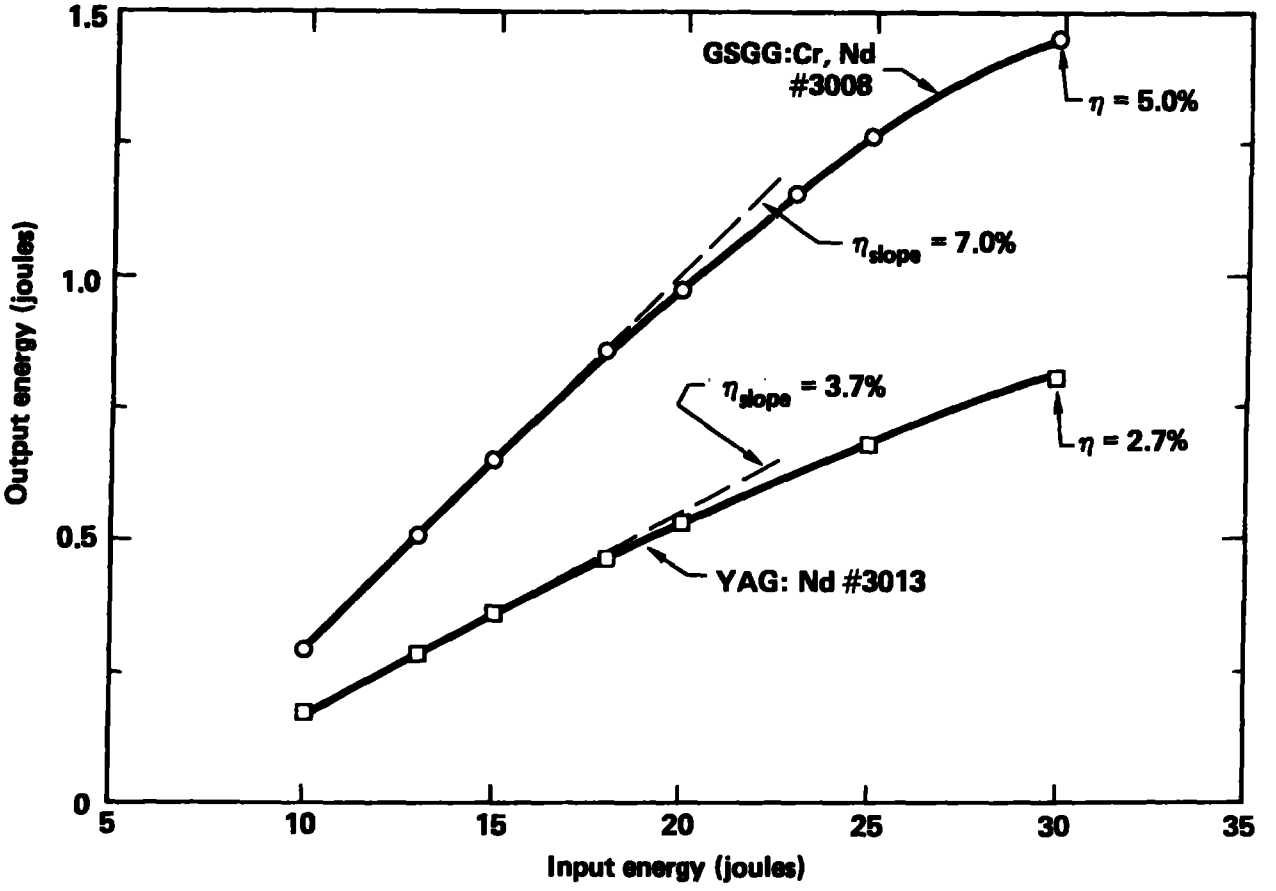

Fig. 10. Free running laser efficiency results for high quality GSGG:Cr,Nd, and YAG:Nd laser rods. A Kigre model #FC-25 laser head was used with a pump pulse width, 3 LC, of 180 μs and a cerium doped quartz lamp. Rod dimensions were 0.25" diameter by 3.0" length. The YAG:Nd doping level is estimated to be 1.5 x 10^{20} cm^{-3}. R_{out} = 49%.

The slope efficiencies are plotted against the insertion loss parameters in Fig. 11 for each rod measured. For GSGG rods with chromium and neodymium concentrations of about $2x10^{20}$ cm^{-3} the average intrinsic slope efficiency was 7.7%. For the YAG rods measured, the average intrinsic slope efficiency was 3.5%. The solid curves in Fig. 11 are plots of Eq. (7) using these two intrinsic slope efficiency values, and R_{out} = 40.8%. The fact that the results for a large number of the GSGG:Cr,Nd rods fall near the upper solid curve over a wide range of insertion loss parameters provides substantial confirmation of the model. It is also apparent from the results displayed in Fig. 11 that the intrinsic lasing efficiency of the GSGG:Cr,Nd rods was not significantly different for chromium ion densities of $1x10^{20}$ and $2x10^{20}$ cm^{-3} (for the same neodymium concentration). In addition, the intrinsic efficiency of the only GGG:Cr,Nd rod tested appears to be comparable to that of the GSGG rods.

X. CONCLUSION

It is clear that the level of losses characteristic of the GSGG laser material available at present is generally much higher than what is typical of commercially grown YAG. Perhaps this is not too surprising, considering the fact that we are in a relatively early stage in the development of GSGG crystal growth technology. In spite of the higher loss levels, however, all of the GSGG laser rods tested have yielded higher lasing efficiency than the best YAG rod. When the losses are accounted for, the intrinsic lasing efficiency of some of the co-doped GSGG rods is found to exceed that of the YAG:Nd rods by more than a factor of 2.

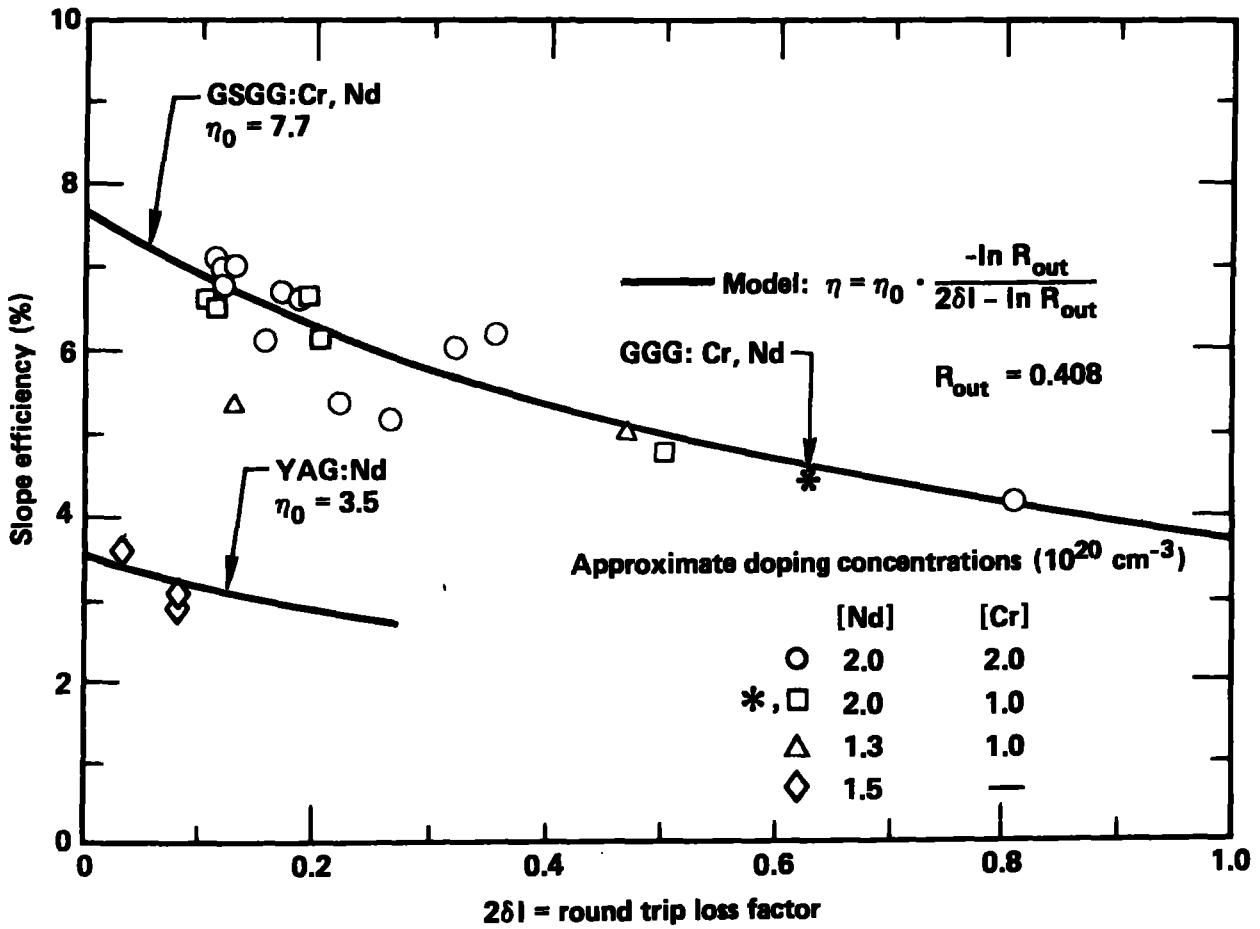

Fig. 11. Free running laser slope efficiency versus resonator insertion loss for a large number of GSGG:Cr,Nd, and YAG:Nd laser rods.

REFERENCES

1. A. G. Avanesov, B. I. Denker, V. V. Osiko, V. G. Ostroumov, V. P. Sakun, V. A. Smirnov, and I. A. Shcherbakov, "Luminescence sensitization and its application to enhance the efficiency of solid-state laser active media," Sov. J. Quantum Electron., 12(4), 421-425 (1982).

2. E. V. Zharikov, V. V. Laptev, V. G. Ostroumov, Yu. S. Privis, V. A. Smirnov, and I. A. Shcherbakov, "Investigation of a new laser active medium in the form of gadolinium scandium gallium garnet crystals activated with chromium and neodymium," Sov. J. Quantum Electron., 14(8), 1056-1062 (1984).

3. A. Beimowski, G. Huber, D. Pruss, V. V. Laptev, I. A. Shcherbakov, and Y. V. Zharikov, "Efficient Cr^{3+} sensitized Nd^{3+}:GdScGa-garnet laser at 1.06 μm," Appl. Phys., B28, 234-235 (1982).

4. D. Pruss, G. Huber, A. Beimowski, V. V. Laptev, I. A. Shcherbakov, and Y. V. Zharikov, "Efficient Cr^{3+} sensitized Nd^{3+}:GdScGa-garnet laser at 1.06 μm," Appl. Phys., B28, 355-358 (1982).

5. E. V. Zharikov, V. A. Zhitnyuk, G. M. Zverev, S. P. Kalitin, I. I. Kuratev, V. V. Laptev, A. M. Onishchenko, V. V. Osiko, V. A. Pashkov, A. S. Pimenov, A. M. Prokhorov, V. A. Smirnov, M. F. Stel'makh, A. V. Shestakov, and I. A. Shcherbakov, "Active media for high-efficiency neodymium lasers with nonselective pumping," Sov. J. Quantum Electron., 12(12), 1652-1653 (1982).

6. E. V. Zharikov, N. N. Il'ichev, V. V. Laptev, A. A. Malyutin, V. G. Ostroumov, P. P. Pashinin, A. S. Pimenov, V. A. Smirnov, and I. A. Shcherbakov, "Spectral, luminescence, and lasing properties of gadolinium scandium gallium garnet crystals activated with neodymium and chromium ions," Sov. J. Quantum Electron., 13(1), 82-85 (1983).

7. E. V. Zharikov, M. B. Zhitkova, G. M. Zverev, M. P. Isaev, S. P. Kalitin, I. I. Kuratev, V. R. Kushnir, V. V. Laptev, V. V. Osiko, V. A. Pashkov, A. S. Pimenov, A. M. Prokhorov, V. A. Smirnov, M. F. Stel'makh, A. V. Shestakov, and I. A. Shcherbakov, "Output characteristics of a gadolinium scandium gallium garnet laser operating in the pulse-periodic regime," Sov. J. Quantum Electron., 13(10), 1306-1307 (1983).

8. P. F. Moulton, "Recent advances in solid state lasers," in the Digest of Technical Papers of the 1984 Conference on Lasers and Electro-Optics (CLEO'84), p. 76, paper WA2 (1984).

9. E. Reed,"A flashlamp-pumped, Q-switched Cr:Nd:GSGG laser," IEEE J. Quantum Electron., QE-21, 1625-1629 (1985).

10. E. V. Zharikov, N. N. Il'ichev, V. V. Laptev, A. A. Malyutin, V. G. Ostroumov, P. P. Pashinin, and I. A. Shcherbakov, "Sensitization of neodymium ion luminescence by chromium ions in a $Gd_3Ga_5O_{12}$ crystal," Sov. J. Quantum Electron., 12(3), 338-341 (1982).

11. W. F. Krupke, M. D. Shinn, J. E. Marion, J. A. Caird, and S. E. Stokowski, "Spectroscopic, optical, and thermo-mechanical properties of neodymium and chromium doped gadolinium scandium gallium garnet," J. Opt. Soc. Am., B3, 102-114 (1986).

12. J. L. Emmett, W. F. Krupke, and W. R. Sooy, "The potential of high-average power solid state lasers," Lawrence Livermore National Laboratory, UCRL 53571, September 1984.

13. C. D. Brandle, "Growth of 3" diameter $Gd_3Ga_5O_{12}$ crystals," J. Appl. Phys., 49, 1855-1858 (1978).

14. F. J. Bruni, Material Progress Corp., Santa Rosa, Ca., private communication.

15. R. G. Warren, Allied Technologies, Synthetic Crystal Products Group, Charlotte, N.C., private communication.

16. F. J. Bruni, "Growth of large GSGG crystals," prepared for the Lawrence Livermore National Laboratory, UCRL-15735, October 8, 1985.

17. F. J. Bruni, "Exploratory crystal growth of laser host oxide crystals," prepared for the Lawrence Livermore National Laboratory, and covering work performed under purchase order number 1342305, interim report, September, 1983.

18. F. J. Bruni, "Exploratory crystal growth of laser host oxide crystals," prepared for the Lawrence Livermore National Laboratory, and covering work performed under purchase order number 1342305, interim report, November 30, 1984.

19. R. F. Belt, R. Uhrin and K. Vermuri, "Research in garnet crystal (GSGG) development," final report under contract DE-AC08-84DP40198, document DOE/DP/40198, availble from NTIS, January, 1985.

20. R. G. Warren, M. H. Randles, D. G. Dawes, C. R. Perleberg, H. M. Wilson, and A. W. Kueny, "Research in gadolinium scandium gallium garnet (GSGG) crystal development," final report under contract DE-AC08-84DP40203, document DOE/DP/40203-1, available from NTIS, July 1985.

21. J. A. Caird, L. K. Smith, and R. E. Wilder, "Measurement of depolarization loss in GSGG:Cr,Nd laser rods," Lawrence Livermore National Laboratories, Internal Memorandum LRD 85-59/4474T, April 1, 1985.

22. K. Kitamura and H. Komatsu, "Optical anisotropy associated with growth striation of yttrium garnet, $Y_3(Al,Fe)_5O_{12}$," Kristall und Technik, 13, 811-816, 1978.

23. C. D. Brandle, D. C. Miller, and J. W. Nielsen, "The elimination of defects in Czochralski grown rare-earth gallium garnets," J. Crystal Growth, 12, 195-200, 1972.

24. K. Kitamura, S. Kimura, Y. Miyazawa, Y. Mori and O. Kamada, "Stress-birefringence associated with facets of rare-earth garnets grown from the melt; a model and measurements of stress-birefringence observed in thin sections," J. Crystal Growth, 62, 351-359, 1983.

25. K. Kitamura, Y. Miyazawa, Y. Mori, S. Kimura, and M. Higuchi, "Origin of difference in lattice spacings between on- and off-facet regions of rare-earth garnets grown from the melt," J. Crystal Growth, 64, 207-216, 1983.

26. J. A. Caird and M. D. Shinn, "1 μm absorption in GSGG:Cr,Nd and calcium content," Lawrence Livermore National Laboratories, Internal Memorandum LRD 85-183/4741T, July 18, 1985.

27. H. L. Tuller, M. D. Shinn, and J. A. Caird, "A model for the anomolous absorption in GSGG:Cr,Nd," Lawrence Livermore National Laboratory, Internal Memorandum LRD 85-242/4906T, September 4, 1985.

28. D. Findlay and R. A. Clay, "The measurement of internal losses in 4-level lasers," Phys. Lett., 20, 277-278, 1966.

29. J. A. Caird and M. D. Shinn, "Advanced crystalline laser materials," 1984 Laser Program Annual Report, Lawrence Livermore National Laboratory, Livermore, Calif., UCRL-50021-84 (1984), pp. 6-75 to 6-83.

30. B. I. Denker, N. N. Il'ichev, G. V. Maksimova, A. A. Malyutin, V. V. Osiko, and P. P. Pashinin, "Efficiency of an Li-Nd-La phosphate glass laser at low pump energies. Free lasing," Sov. J. Quantum Electron., 11, 965-967, 1981.